Multiply Nested Regional Climate Simulation for Southern South America: Sensitivity to Model Resolution

MAISA ROJAS

Department of Geophysics, University of Chile, Santiago, Chile

ABSTRACT

Results are reported from two 5-month-long simulations for southern South America using the fifth-generation Pennsylvania State University–NCAR Mesoscale Model (MM5). The periods of simulation correspond to May–September 1997 and 1998, which were anomalously wet and dry winters for central Chile, respectively. The model setup includes triply nested, two-way-interacting domains centered over the eastern South Pacific and the western coast of southern South America, with horizontal grid intervals of 135, 45, and 15 km. Boundary conditions are provided from NCEP–NCAR reanalyzed fields. The analysis focuses on two subregions of central Chile (30°–41°S). Region 1 (32°–35°S), which is where the observed interannual precipitation differences are largest, is topographically very complex, with a mean height of the Andes Cordillera around 4500 m. Region 2 (35°–39°S) has relatively smooth terrain, as the mean height of the Andes drops to 3000 m. Station precipitation and temperature data are used for model validation. The model exhibits a negative temperature bias (from 2° to 5°C), as well as a positive precipitation bias (40%–80%). This precipitation bias can be partially explained by a positive moisture bias over the ocean in the model. In addition, these biases are highly correlated to the representation of terrain and station elevation in the model. The highest-resolution domain has the smallest precipitation bias for low-elevation stations, but a large positive bias at high altitudes (up to 300%). It also has a better representation of the spatial distribution of the precipitation, especially in region 1, where topography has a larger impact on the precipitation. Overall, the model domain with highest resolution best reproduces the observed precipitation and temperature, as well as the interannual differences. However, this study also shows that large improvements in the simulations of the surface variables are obtained when downscaling from 135 to 45 km, but much smaller improvements are found when downscaling from 45 to 15 km. These simulations represent the first effort in simulating seasonal precipitation in this topographically complex region of the Southern Hemisphere.

1. Introduction

The study of climate on seasonal and longer time scales with regional climate models has become increasingly more affordable and is being tested in a number of very diverse regions around the world (e.g., Arnell et al. 2003; Seth and Rojas 2003; Giorgi et al. 2004; Small et al. 1999). In the case of Chile, the country is highly dependent on precipitation for agriculture and hydropower energy production, but the territory is topographically very complex, making it a challenge for numerical climate modeling.

The western coast of South America south of 15°S is a narrow stretch of land between the Pacific Ocean and the Andes Cordillera. From north to south the climates vary from the extremely dry Atacama Desert to the very wet western Patagonia region. The region of interest in this study is central Chile (30°–41°S), which is economically very important for Chilean agriculture activity (García-Huidobro et al. 2001) and is home to over 80% of the country's population (Instituto Nacional de Estadísticas 2005). Annual rainfall in the region varies from around 100 to 2000 mm (Miller 1976), and originates mainly from cold fronts associated with migratory low pressure systems embedded in the midlatitude westerlies (Fuenzalida 1982). Cutoff lows contribute between 5% and 10% to the annual rainfall (Pizarro and Montecinos 2000). The influence of the Atlantic Ocean is almost completely blocked by the Andes.

The winter precipitation regime is explained by the seasonal changes of the large-scale circulation. The region is under the direct influence of the South Pacific

Corresponding author address: Maisa Rojas, Dept. of Geophysics, University of Chile, Blanco Encalada 2002, Santiago, Chile.
E-mail: maisa@dgf.uchile.cl

anticyclone (SPAC), whose climatological position is centered around 30°S during austral summer and around 25°S in winter, allowing fronts to reach the continent farther north, thus bringing precipitation to the region (Rutllant and Fuenzalida 1991).

Although the synoptic conditions are responsible for precipitation events in the region, by frontal activity reaching the continent from the Pacific Ocean, it is the interplay with the orography that determines the spatial distribution of the precipitation. The geography of central Chile is characterized by a mountainous range at the coast, with its highest points reaching about 1500 m; an intermediate valley, about 40–50 km wide; and, at the eastern end, the Andes Cordillera, which has peaks of up to 6000 m in northern and central Chile. At around 35°S, the altitude of the Andes starts to decline to a mean level of about 3000 m.

The relationship between central Chilean rainfall and the El Niño–Southern Oscillation (ENSO) has long been established (Aceituno 1988), with a general pattern of relatively wet winters during El Niño years and relatively dry winters during La Niña years. Positive sea surface temperature (SST) anomalies in the western equatorial Pacific produce anomalous atmospheric heating in the region, which triggers wave trains across the Pacific that are then linked to enhanced blocking activity over the Bellingshausen Sea (90°W). The SST anomalies also change the large-scale circulation of the Walker cell with a weaker and farther-northward-displaced SPAC. These factors in turn allow more rainfall events to reach central Chile. During the cold phase of ENSO (La Niña events), the SPAC is more persistent and farther south from its climatological position, thus deflecting the midlatitude perturbations farther south, resulting in relatively dry winters in central Chile.

This relationship has been further explored in Montecinos and Aceituno (2003), who showed that ENSO-related rainfall variability is highly seasonally dependent in central Chile, with most significant relationships between SST anomaly and precipitation occurring in winter [June–August (JJA)] from 30° to 35°S, during late spring [October–November (ON)] between 35° and 38°S, and during summer [January–March (JFM)] from 38° to 41°S.

The question of how higher horizontal resolution influences the simulation of precipitation processes when orographic effects are important is addressed in this paper. Two 5-month-long simulations using the fifth-generation Pennsylvania State University–National Center for Atmospheric Research (PSU–NCAR) Mesoscale Model (MM5) model driven by National Centers for Environmental Prediction–National Center for Atmospheric Research (NCEP–NCAR) reanalysis fields have been performed to simulate the winter (May–September) 1997 and 1998 seasons. These correspond to a wet El Niño year and a very dry La Niña year (Departamento de Geofísica 2005). The sensitivity of the simulated precipitation to model horizontal resolution in two extreme seasons is evaluated with three nested domains.

The rest of the paper is organized as follows: section 2 gives a brief description of the model and data used in the study, section 3 presents the results, section 4 discusses the results, followed by the summary and conclusions in section 5.

2. Model setup and data

a. MM5

The MM5 model (Dudhia 1993) is used to run two 5-month-long simulations centered over southern South America. The parameterization schemes used to resolve the subgrid physics include the following: the Medium-Range Forecast planetary boundary layer (Troen and Mahrt 1986), the Kain–Fritsch convective parameterization scheme (Kain and Fritsch 1993), the Oregon State University land surface model (Chen et al. 1996), the Community Climate Model 2 radiative parameterization scheme (Hack et al. 1993), shallow convection, and the Dudhia simple ice scheme for cloud microphysics (Dudhia 1989).

Figure 1 is the nested domain setup for the model experiments used in this study. With a grid spacing of 135 km, domain 1 includes the SPAC region, which plays a relevant role in the central Chilean climate. Domain 2 has a grid size of 45 km, and domain 3 has a grid size of 15 km and is fine enough to resolve the intricate topography of Chile. The model has 30 vertical levels with a top at 100 hPa. The model runs in a two-way nesting mode so that the smaller domain feeds back into the larger domains. The initial conditions and lateral boundary conditions are provided from 6-hourly NCEP–NCAR reanalysis fields (Kalnay et al. 1996).

b. Station data

One-hundred-and-twenty stations with daily precipitation data and 85 stations with daily extreme temperature data were available for validating model output. These data were provided by the National Meteorological Service, were selected for having no missing data for the period of simulation, and were quality controlled. In addition, 95 stations from the National Water Administration, with daily precipitation data at latitudes between 32° and 35°S, are included. Also used in the

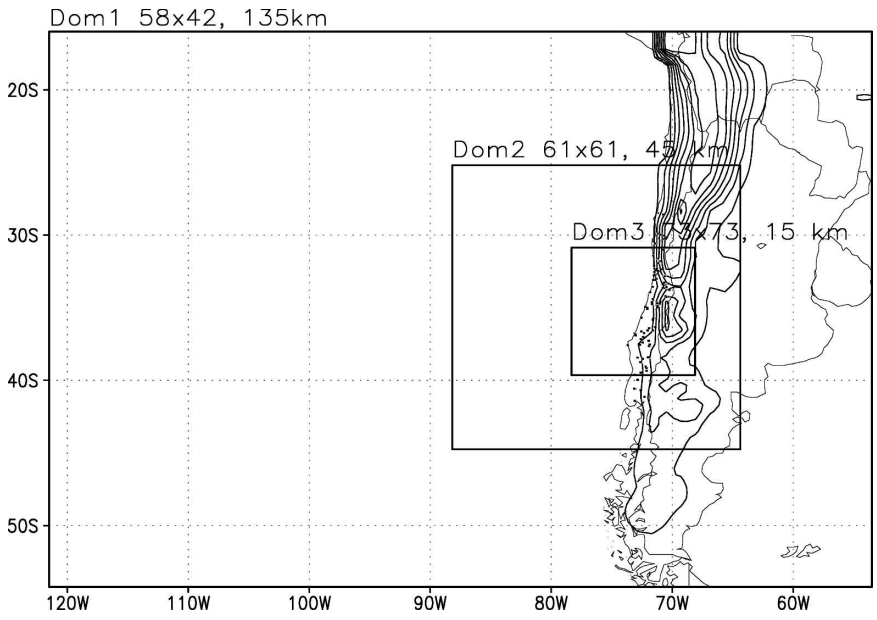

FIG. 1. MM5 configuration: Three nested models domains and the resolution of each domain. The dots represent the location of available station data.

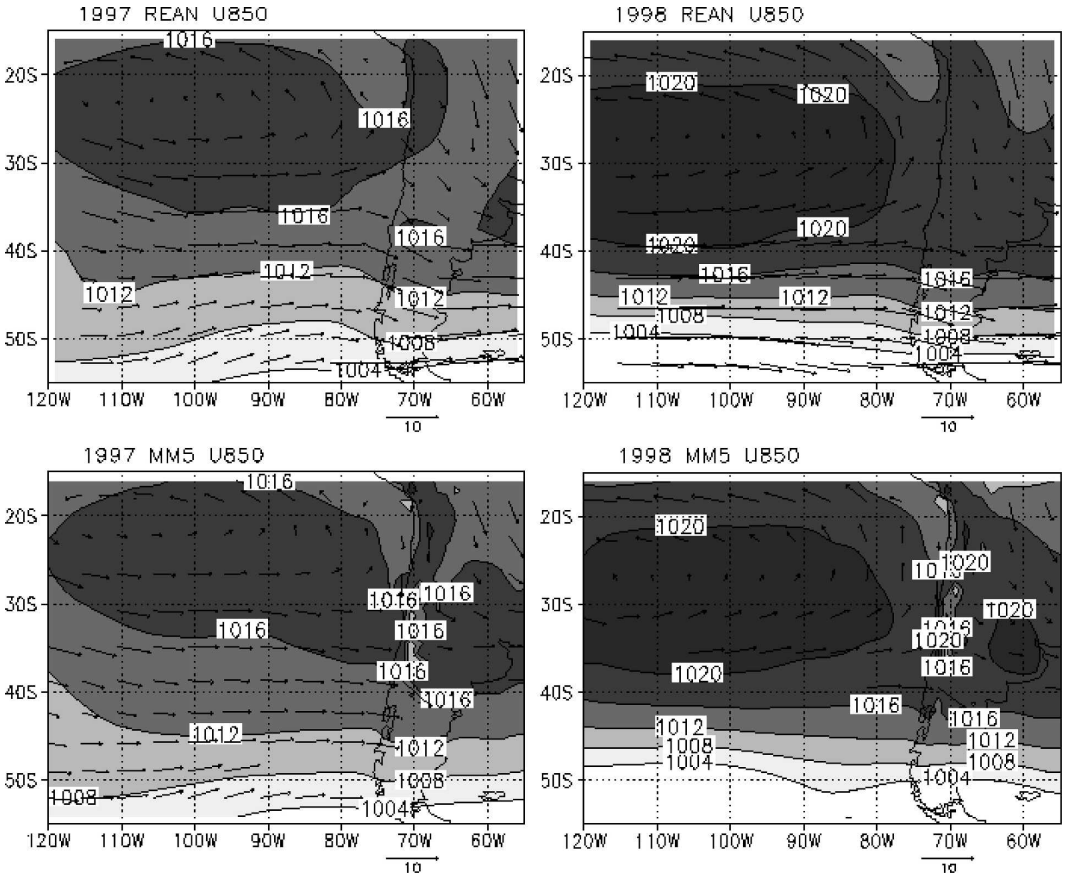

FIG. 2. Seasonal mean MJJAS SLP and 850-hPa winds from (top) reanalysis and (bottom) MM5 domain 1 for (left) 1997 and (right) 1998.

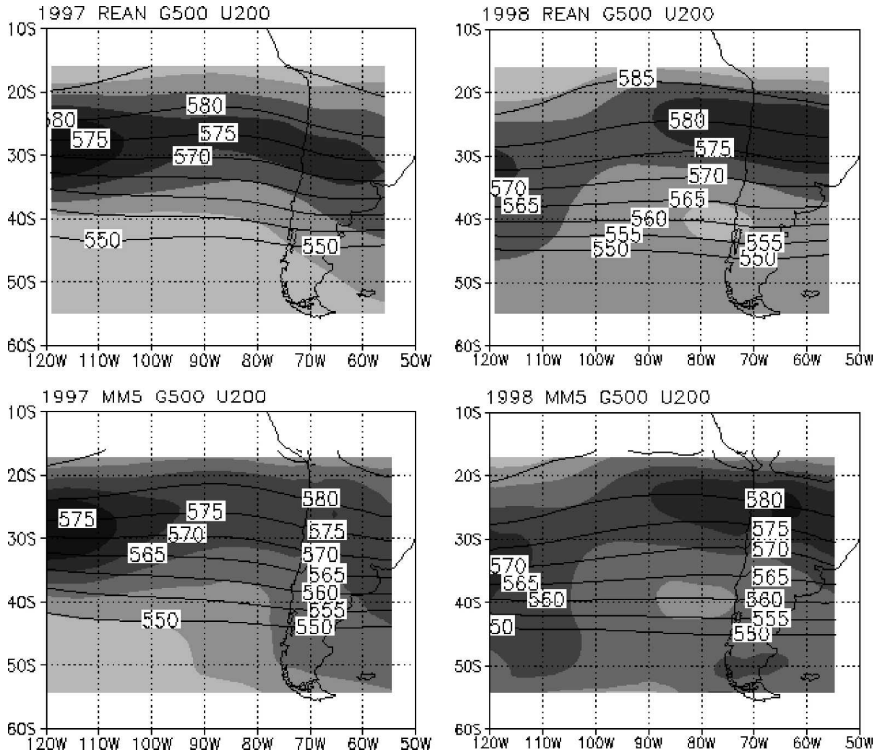

FIG. 3. Seasonal mean (MJJAS) 500-hPa height field (line contours) and 200-hPa winds (filled contours), from (top) reanalysis and (bottom) MM5 domain 1 for (left) 1997 and (right) 1998.

validation are profiles of temperature and water vapor mixing ratio from radiosonde observations. The radiosonde data come from Global Telecommunication System station 85586, which is located at 32.5°S and 71.5°W. Finally, the Global Precipitation Climatology Project (GPCP) Merged Satellite–Gauge Dataset (Adler et al. 2003) is used for validating precipitation. GPCP precipitation is a gridded analysis compiled by combining gauge measurements and satellite estimates.

3. Results

In the following sections simulated circulation, temperature, and precipitation are evaluated, with a focus on central Chile in the three domains. In all cases when comparing model results with station data, the model fields were interpolated onto station data location. Biases between model and station data are calculated as the absolute difference between them.

a. Circulation

The seasonal mean [May–September (MJJAS)] circulation at 850 hPa is dominated by the SPAC. Figure 2 shows the seasonal mean sea level pressure (SLP) and 850-hPa winds from the reanalysis and MM5 simulations for 1997 and 1998. The reanalysis SLP for 1997 shows a weaker SPAC located farther northward and for 1998 the SPAC is stronger and located farther westward with stronger low-level winds around the SPAC and stronger westerlies south of 45°S. These patterns are well captured by the MM5, although the 1998 SPAC in the MM5 is weaker than in the reanalysis, with winds around this high pressure cell accordingly slower, especially the westerlies between 20° and 25°S.

Figure 3 shows the seasonal mean 500-hPa height field in contours and 200-hPa winds in shaded contours from the reanalysis and MM5 domain 1, for 1997 and 1998. The reanalysis shows a 500-hPa height field in 1997 that is less zonal than in 1998, especially at the western border of the domain. This is well simulated by MM5. The jet stream in 1997 was stronger and located farther south in comparison with 1998. The representation of the jet in MM5 is correctly positioned, but is less intense than in the reanalysis in both years, especially in 1997.

b. Temperature

Daily maximum and minimum temperature were calculated from 6-hourly model 2-m temperature output.

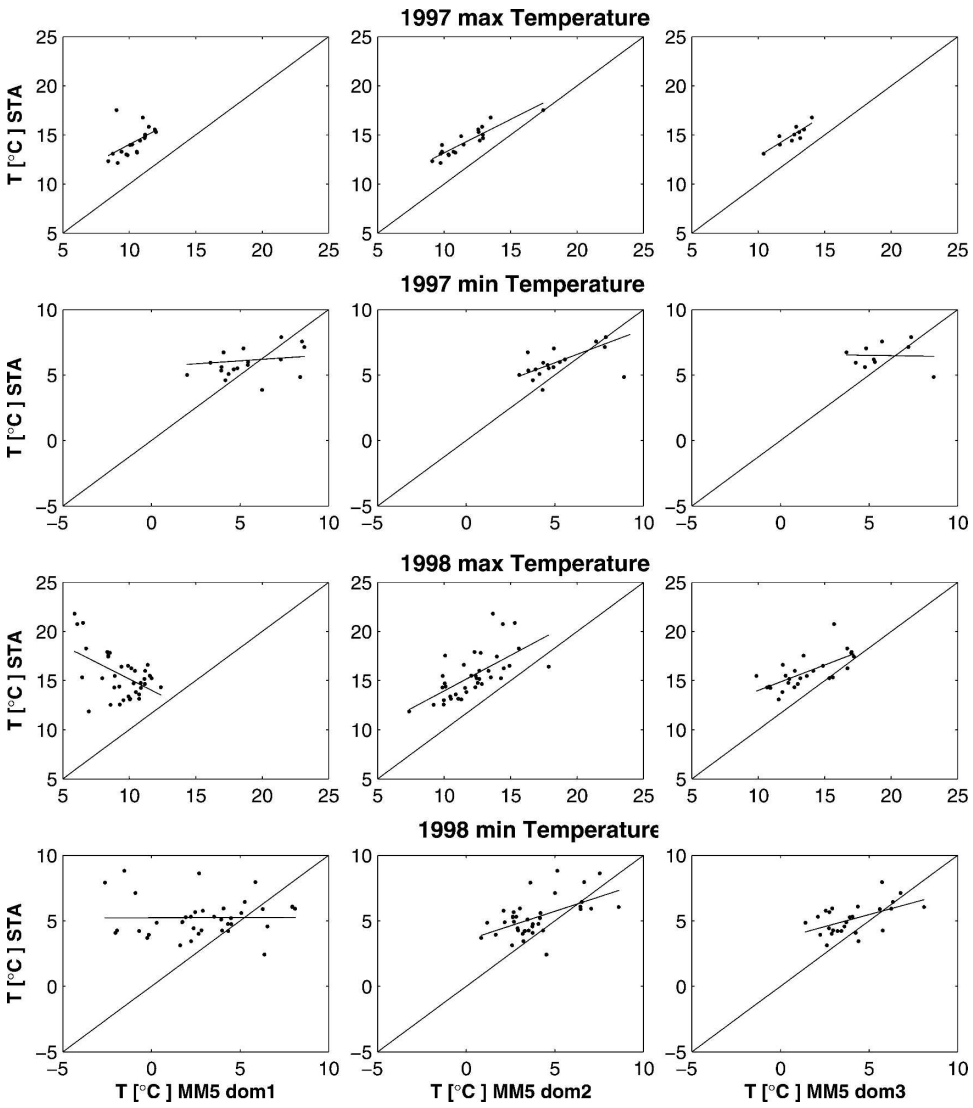

FIG. 4. Temperature correlation plotted as station data vs MM5 for maximum and minimum temperatures in 1997 and 1998.

Figure 4 shows the temperature scatterplot between the seasonal mean station data and the simulations of the three MM5 domains, for maximum and minimum temperatures in both years. The figure indicates that the model underestimates (to different degrees) the temperature in all cases. The relationships between modeled and observed 2-m temperatures are equally consistent in 1997 and 1998, with a linear relationship for domains 2 and 3. In contrast, observed and modeled temperatures are almost uncorrelated for domain 1.

As the calculation of maximum and minimum temperature was done from 6-hourly model output data, sampling the whole daily temperature range in the model would certainly give a smaller error. However, these results can be corrected, as it is found that the temperature bias is correlated to the differences between station and model height. This is shown in Fig. 5 for the MM5 domain 1. There is a linear relation (correlation coefficients -0.7) between the temperature difference of the station and the model domain 1 and the difference between the station and the model height. For the minimum temperatures, the fitted straight line passes through the origin. The slope of those lines (indicated in the figure) can therefore be used to correct the modeled temperature, as an empirical lapse rate. The values are not far off from the atmospheric lapse rate of $0.0065°\text{C m}^{-1}$. Linear relationships are also obtained for model domains 2 and 3 (not shown).

Table 1 shows the correlation coefficient R, bias, and

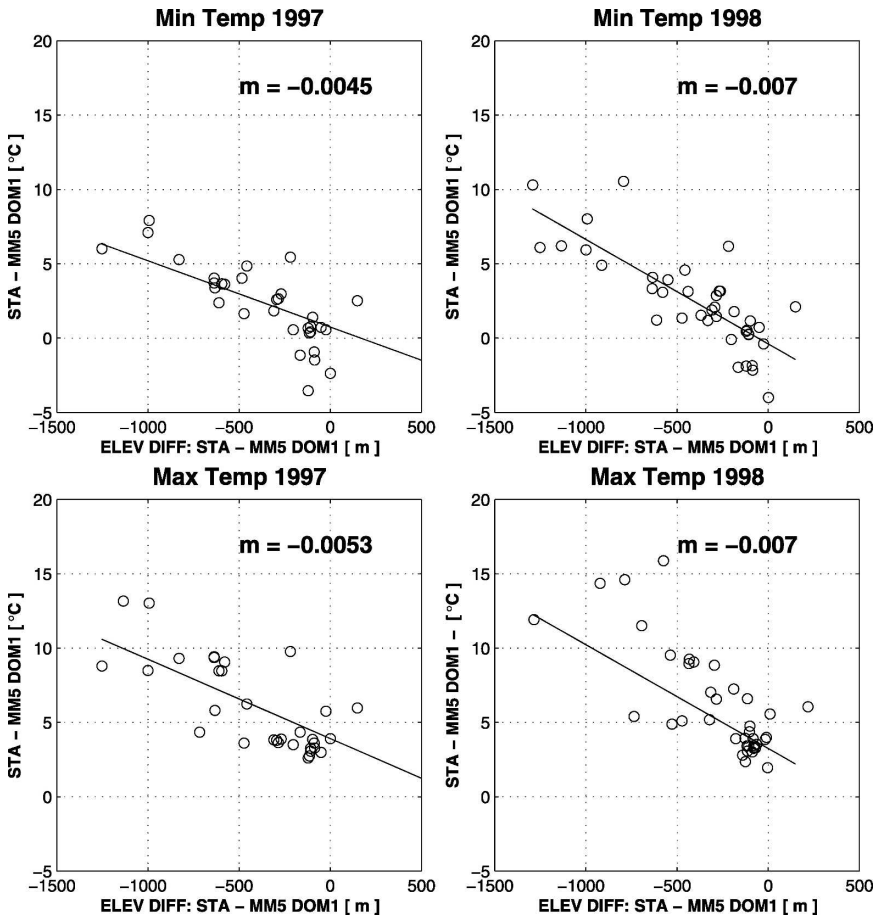

FIG. 5. Scatterplot between temperature difference vs difference in station and model height for MM5 domain 1 for (top) minimum temperature, (bottom) maximum temperature, (left) 1997, and (right) 1998.

standard deviation (Std) between the seasonal mean maximum and minimum observed temperatures and the three MM5 domains, and shown in parenthesis are the values for the temperature corrected by the empirical lapse rate obtained from the relationship between the differences of the station and the modeled temperatures and the differences of the station and the modeled heights. The biases for the maximum temperatures are higher than for the minimum temperatures. Domain 1 exhibits the largest bias, ~6° and ~2.5°C, and domains

TABLE 1. Seasonal mean temperature *T* correlation *R*, bias, and standard deviation (Std) for MM5 domains 1, 2, and 3. In parentheses are the values for the temperatures corrected by the slope of the relationship between the differences in the station and modeled temperatures and the differences between the station and modeled heights, as shown in Fig. 5 for MM5 domain 1.

		1997		1998	
Domain		Max *T*	Min *T*	Max *T*	Min *T*
1	*R*	0.2 (0.62)	−0.1 (0.64)	−0.5 (0.26)	0.00 (0.28)
	Bias	−5.8 (−3.9)	−2.1 (−0.7)	−6.1 (−3.2)	−2.4 (0.3)
	Std	2.7 (1)	1.3 (0.3)	3.3 (1.9)	1.4 (0.9)
2	*R*	0.70 (0.88)	0.66 (0.75)	0.65 (0.82)	0.55 (0.6)
	Bias	−3.6 (−1.8)	−1.3 (0.0)	−3.3 (−1.5)	−1.3 (0.0)
	Std	0.6 (0.9)	0.8 (0.8)	0.6 (1.0)	1.0 (1.1)
3	*R*	0.72 (0.9)	0.40 (0.4)	0.68 (0.81)	0.53 (0.55)
	Bias	−2.8 (−1.9)	−0.9 (−0.6)	−2.5 (−1.7)	−1.1 (−1.2)
	Std	0.5 (0.2)	1.1 (1.0)	1.0 (1.0)	1.0 (1.0)

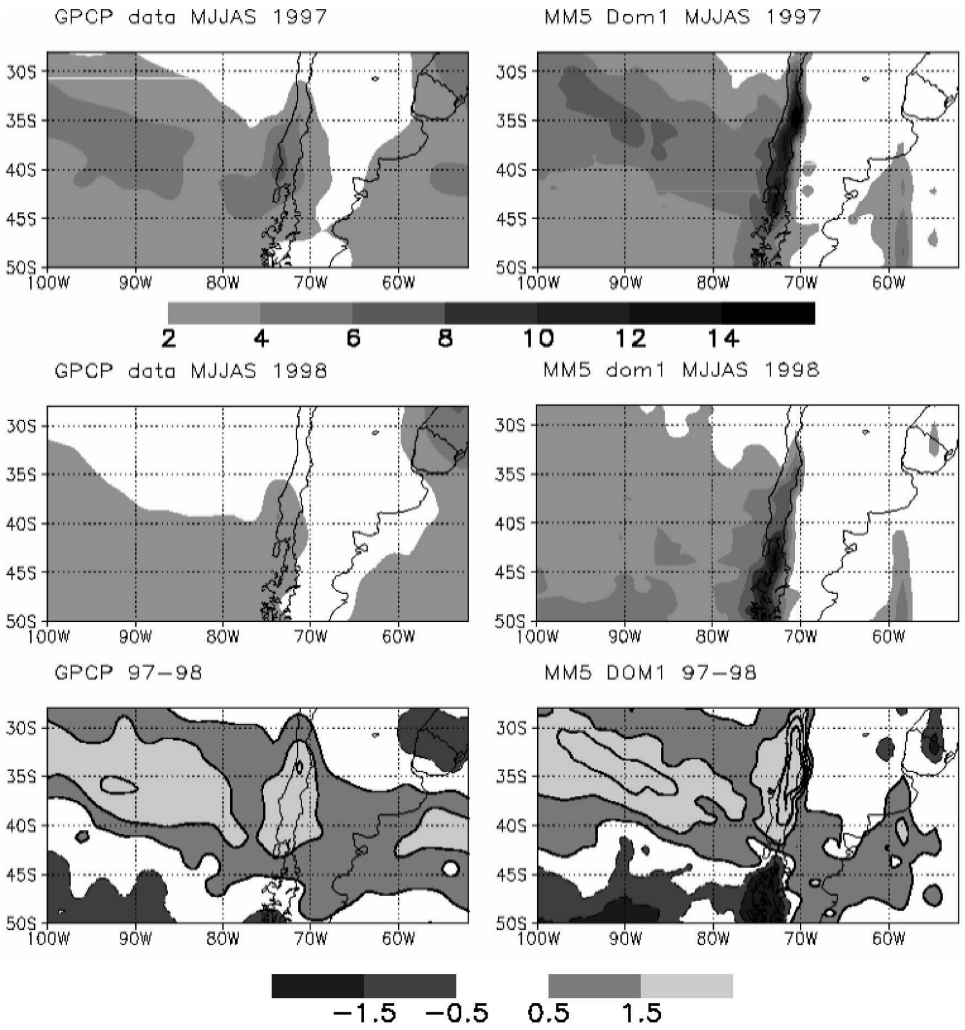

FIG. 6. Seasonal mean (MJJAS) precipitation from (left) GPCP and (right) MM5 domain 1 for (top) 1997, (middle) 1998, and (bottom) 1997 − 1998 differences.

2 and 3 are comparable, ~3°C, with the smallest values and standard deviation for domain 3, ~2.5° and ~1°C for maximum and minimum temperatures, respectively. The corrected temperatures show better correlation coefficients and smaller biases.

c. *Precipitation*

Figure 6 shows the seasonal mean precipitation for 1997 and 1998, for the GPCP dataset, MM5 domain 1, and the 1997 − 1998 differences. The patterns of precipitation through the southern South American sector and the adjacent ocean in the domain are well represented in the model in each year, as are the interannual differences. There are positive differences throughout the domain in a band in the NW–SE direction, and negative difference in Uruguay and south of 40°S.

Focusing on central Chile and comparing with the available station data, Fig. 7 shows the percentage ratio $[(\langle PP_{98}\rangle/\langle PP_{97}\rangle) \times 100]$ of the seasonal mean precipitation of the station data, and the three MM5 domains, where PP_{98} and PP_{97} are the amount of precipitation that fell in 1998 and 1997, respectively, and the angle brackets indicate the May–September mean. In Fig. 7a two subregions can be clearly identified: from 32° to 35°S (hereafter region 1) the seasonal mean rainfall in 1998 represents only 9% of that which fell in 1997 (large black dots in the figure), whereas for the region from 35° to 39°S (hereafter region 2) the 1998 precipitation represents 47% of that which fell in 1997 (smaller dark gray dots in the figure).

The three MM5 domains capture the precipitation pattern, and the two subregions are also evident from the figure. However, in region 1 the percentage ratio amounts only to 33%, 29%, and 27% in domains 1, 2,

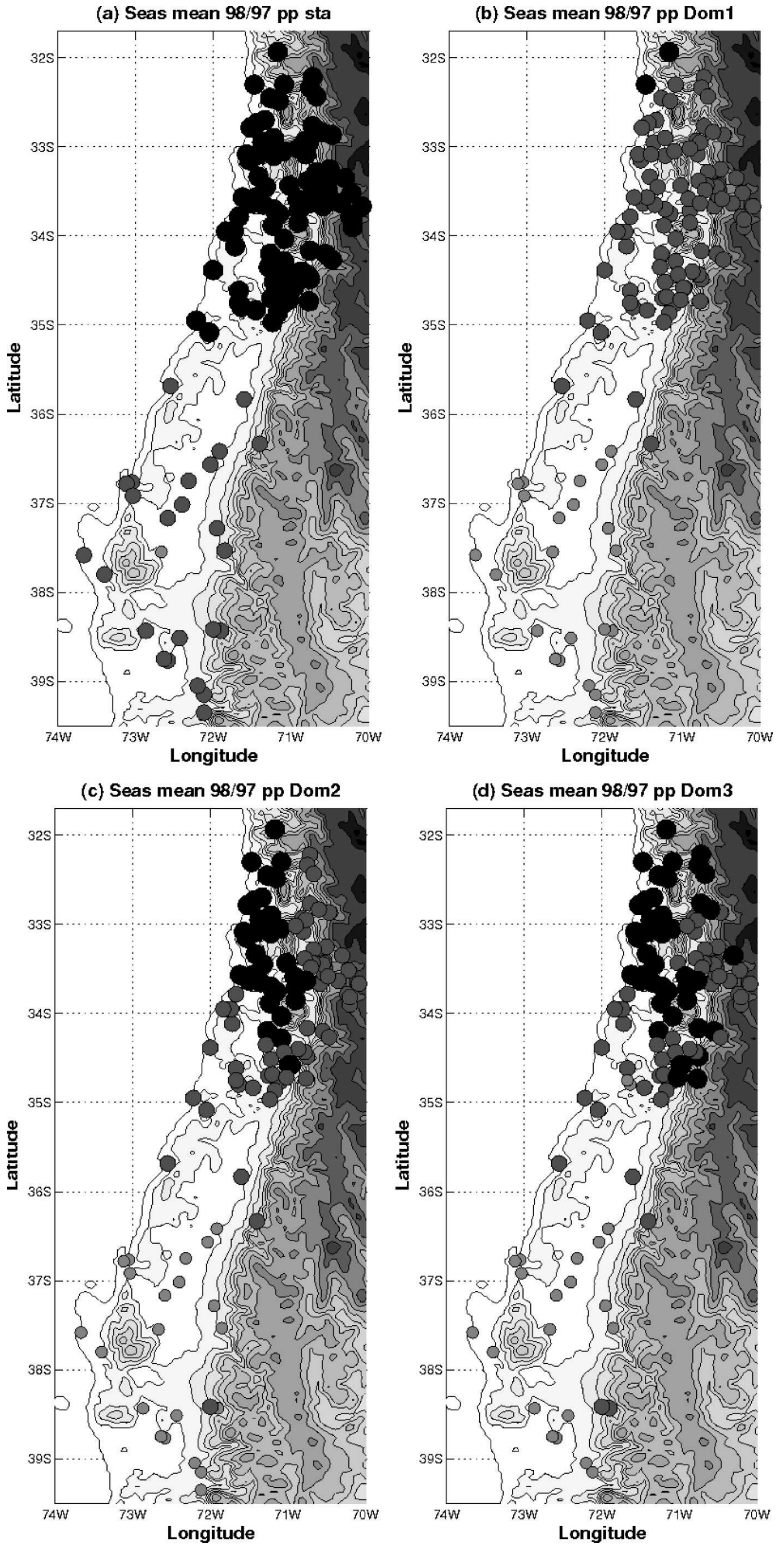

FIG. 7. Percentage ratio of total seasonal (MJJAS) rainfall, $(\langle PP_{98}\rangle/\langle PP_{97}\rangle) \times 100$, for MM5 precipitation interpolated on station data location: (a) station data, (b) MM5 domain 1, (c) MM5 domain 2, and (d) MM5 domain 3. $(\langle PP_{98}\rangle/\langle PP_{97}\rangle) \times 100 \leq 30\%$ (large black dots), $30\% < (\langle PP_{98}\rangle/\langle PP_{97}\rangle) \times 100 \leq 60\%$ (smaller dark gray dots), and $60\% < (\langle PP_{98}\rangle/\langle PP_{97}\rangle) \times 100 \leq 90\%$ (smaller light gray dots).

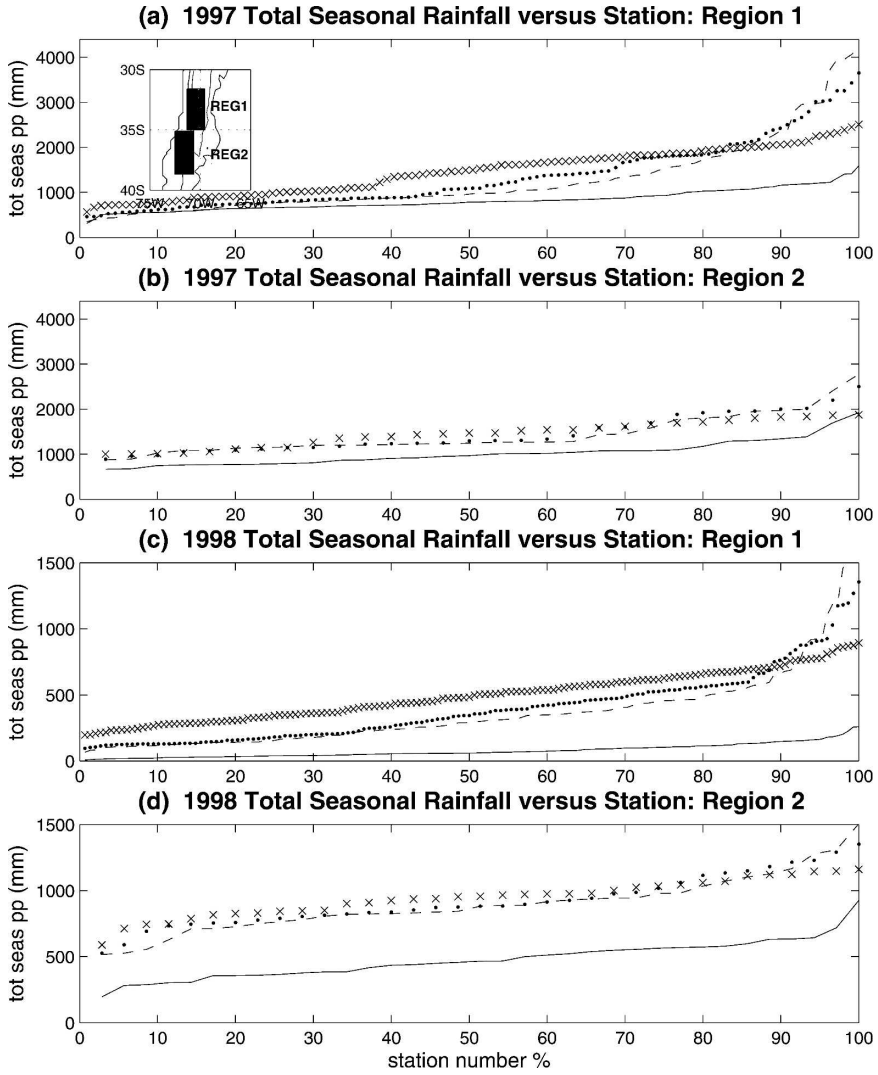

FIG. 8. Increasing total seasonal precipitation amounts vs station number (%): (a) 1997 region 1, (b) 1997 region 2, (c) 1998 region 1, and (d) 1998 region 2 for station data (solid line), MM5 domain 1 (crosses), MM5 domain 2 (dotted line), and MM5 domain 3 (dashed line).

and 3, respectively; and in region 2 the differences are 65%, 63%, and 62% in domains 1, 2, and 3, respectively. The figures also show that the model stations closer to the cordillera show smaller interannual differences (especially in region 1, where smaller, dark gray dots are seen instead of the larger black dots).

The overestimated precipitation in MM5 can also be seen in Fig. 8, which shows the total seasonal rainfall amount per station sorted in increasing order of rainfall amount, versus number of stations (%), by year and region. The solid lines correspond to station data, crosses are used for domain 1, dotted lines for domain 2, and dashed lines for domain 3. For example, in 1997 for 85% of the stations in region 1, domain 3 has the smallest precipitation bias with respect to the station data (curve closest to the station curve), while domain 1 has the largest bias. In addition, for only the last 5% of the stations is the overprediction of rainfall in MM5 domain 3 extremely large (over 200%). A similar behavior is observed in 1998. Region 2, however, shows a nearly constant bias in all three domains and in both dry and wet years. It is also apparent from Fig. 8 that the differences between domain 2 and domain 3 are small compared with their differences with domain 1. The last 5% of the stations, with the largest rainfall amounts of domains 2 and 3 in both years, all correspond to stations above 1200 m, and hence Fig. 8 indicates that the rainfall bias in the model depends on topographic variations represented in each model domain.

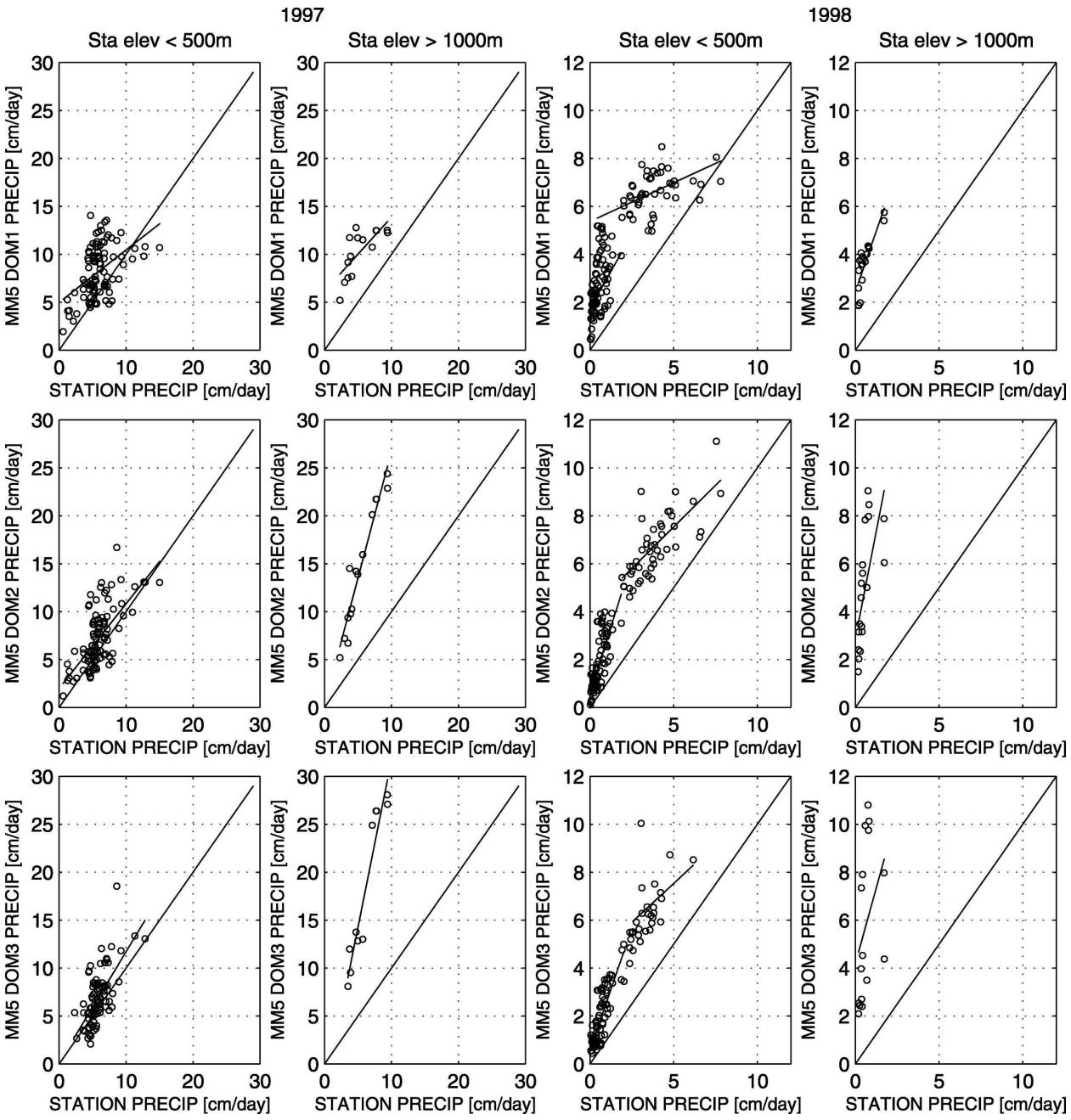

FIG. 9. Scatterplot between station and modeled precipitation for stations below 500-m height and stations above 1000 m from (top) MM5 domain 1, (middle) MM5 domain 2, and (bottom) MM5 domain 3.

To illustrate this, Fig. 9 shows scatterplots between station and modeled precipitation divided into two categories: stations whose elevation are below 500 m and stations above 1000 m. Differences are observed among these categories as well as among both years. In 1997, the correlation between the observed and modeled precipitation is very high (correlation coefficients of 0.5, 0.67, and 0.67 for domains 1, 2, and 3, respectively) with small biases for the stations below 500 m (40%, 25%, and 17% for domains 1, 2, and 3, respectively), especially in domains 2 and 3. Large biases are seen at stations above 1000 m. A similar situation is true in 1998, but here, additionally, there seems to be a larger overestimation of light precipitation events, at least in the low-elevation stations (see the two lines fitted for correlation for stations below 500 m in 1998). In 1998 the

TABLE 2. Seasonal total precipitation (mm).

	Region 1				Region 2			
	Station	Domain 1	Domain 2	Domain 3	Station	Domain 1	Domain 2	Domain 3
1997 total	818	1456	1352	1277	1026	1453	1452	1434
1997 coast	700	735	626	610	1045	1051	1115	1189
1997 interior	830	1529	1425	1344	1020	1575	1555	1508
1998 total	76	493	399	366	477	944	921	895
1998 coast	87	272	214	203	507	757	809	856
1998 interior	75	509	412	377	471	982	944	903

precipitation biases are 480%, 330%, and 300% for domains 1, 2, and 3, respectively, and for larger precipitation events, the biases are 86%, 71%, and 80%, respectively.

Figure 8 showed that the precipitation bias in the model is nearly constant with the precipitation amount, except for those stations at higher altitudes (above 1000 m), where the differences become very large. The relationship between the observed and modeled precipitation, with respect to the spatial distribution in both years, is further analyzed in Table 2. The total seasonal precipitation for both years for the two subregions are given, and the precipitation totals by stations are divided into two groups: coastal stations and interior stations. In region 1 in 1997 there is more precipitation in the interior valley stations than for those at the coast, and in 1998 the opposite is true. In region 2 a different pattern is observed: in both years it rains more at the coastal stations than in the interior. In all domains and in both years, more rain was simulated by MM5 in the interior valleys than at the coast.

To analyze the simulation of the daily precipitation, Fig. 10 shows latitude–time cross sections of precipitation for 1997 and 1998, for station data from 32° to 39°S at ~72°, and the three MM5 domains. Overall, the simulated rainfall events agree remarkably well with the observed time evolution of events. The model captures the individual precipitation events. A closer inspection reveals that, especially for 1998, the latitudinal extent of some of the simulated events reaches farther north than is observed. This model error is partially improved in MM5 domains 2 and 3. To help in visualizing this improvement, in the bottom panels of the figure dots indicate days when the precipitation difference between model domain 1 and domain 3 are larger than 5 mm day^{-1} in the region north of 35°S, thus indicating situations when the precipitation in MM5 domain 3 improves upon MM5 domain 1. A time series of the mean precipitation for each subregion (not shown) shows closer correspondence to the observations in MM5 domains 2 and 3. As illustrated in Fig. 10, in addition to some correction in the precipitation amount, the spatial distribution is improved due to higher model resolution.

4. Discussion

As was mentioned in the previous section, the interannual differences in station precipitation data clearly show two subregions: from 31° to 35°S and from 35° to 39°S, which coincide with a decline in the altitude of the Andes at 35°S (from a mean altitude above 4500 m to about 3000 m). In the first region, the seasonal mean rainfall in 1998 amounts to 9% of the seasonal rainfall in 1997, whereas in region 2 the 1998 rainfall total represents 47% of the 1997 rainfall. This extremely dry winter in region 1 is only partially simulated by MM5. In region 1, the rainfall simulated in 1998 amounts to 27%, 29%, and 33% of that in 1997 (for domains 3, 2, and 1, respectively). In region 2 the station data show 47% less rainfall in 1998, and MM5 simulates 62%, 63%, and 65% for domains 3, 2, and 1, respectively.

The incorrect rainfall amount in region 1 may be attributed to two factors. First, rain is produced in the region because northeastward-moving fronts in the model reach farther north than is observed in the reanalysis fields. The second situation corresponds to rainfall at the eastern slope of the Andes, which is not observed. In the first situation, the model synoptic fields show troughs that are deeper and located farther northward at the surface in comparison with reanalysis fields for the same events. These errors are reflected in the weaker than observed seasonal mean SPAC in 1998 (see Fig. 2).

The large precipitation bias at high-altitude locations is related to a more accurate representation of the Andes in model domains 2 and 3, and the corresponding steeper mountain slopes. This has an impact on the divergence of the horizontal wind flow, the vertical velocity, and hence the precipitation on the upslope side and at the top of the Andes. An examination of these variables for cases when the model produces spurious precipitation events in the cordillera revealed that although the horizontal winds are similarly simulated in

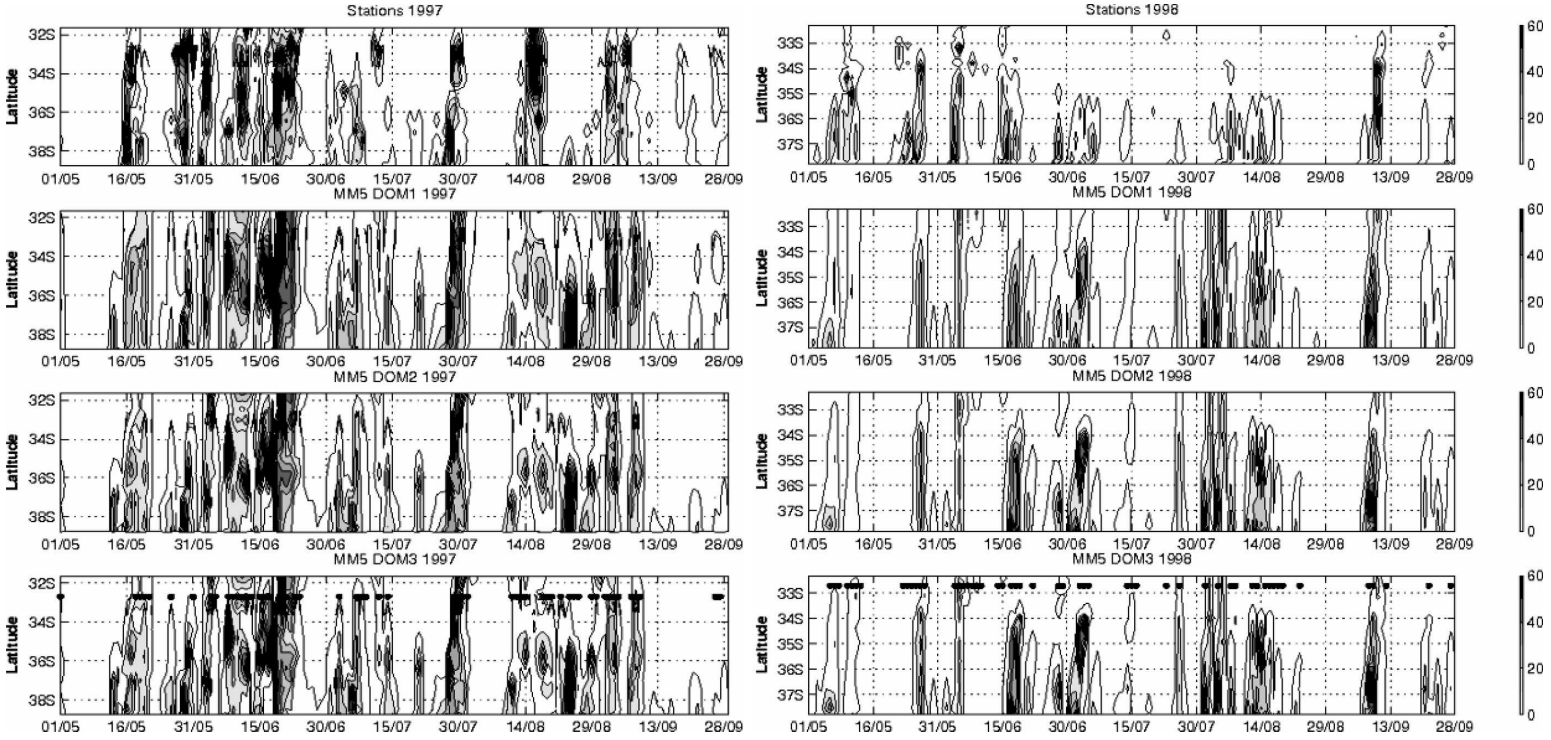

FIG. 10. Time series of daily precipitation vs latitude at ~72°W during (left) 1997 and (right) 1998. Station data are shown in the top panels; upper middle, lower middle, and bottom panels are for MM5 domains 1, 2, and 3, respectively. The dots in bottom panels indicate days when precipitation north of 35°S fulfills MM5 domain 1 − MM5 domain 3 < 5 mm day^{-1}.

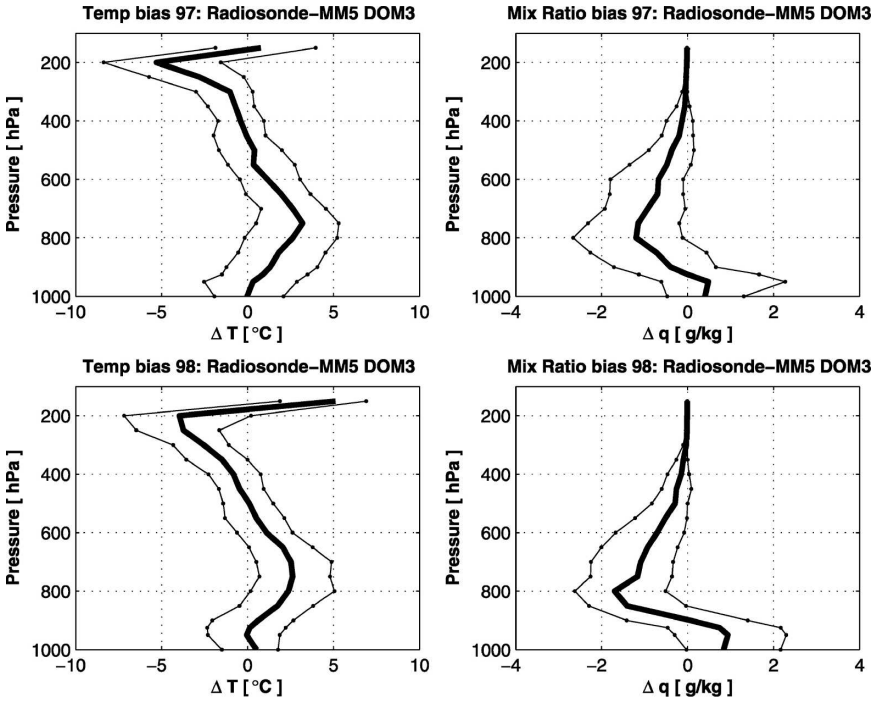

FIG. 11. (left) Seasonal mean radiosonde profile minus MM5 domain 3 profile of temperature and (right) water vapor mixing ratio. In each panel, the thick middle line corresponds to the median of the bias (50th percentile) and the thin left and right lines to the 25th and 75th percentiles, respectively.

all three MM5 domains, it is in domains 2 and 3 that the divergence of the winds increases when reaching the Andes, as stronger upward vertical velocity are seen and intense precipitation is produced. This situation was also observed by Grell et al. (2000) for precipitation over the Alps simulated with MM5.

Regardless of the overestimation of the rainfall in 1998, the model has a systematic error in precipitation amounts. A possible contribution to this bias could be larger water vapor content in the model. In region 1 there is one site where radiosondes are routinely launched.

Figure 11 compares modeled temperature and water vapor mixing ratio q with the results from the radiosondes. The figure shows a positive q bias ($\sim$1 g kg^{-1}) within the boundary layer in the model. The thick middle line corresponds to the 50th percentile of the seasonal mean, and the thinner left and right lines to the 25th and 75th percentile, respectively. The profiles are similar for 1997 and 1998, although a slightly larger 50th percentile bias is seen in 1998, with smaller spread (25th and 75th percentiles). The spatial distribution of this bias is evaluated by comparing reanalysis temperatures and relative humidity with the modeled values (not shown). Comparing these variables at different vertical levels reveals that from the surface up to around 800 hPa the model has much higher values of water vapor than the reanalysis fields, in both years and with even higher values in 1998. The higher values of water vapor, which is available as moisture, are transformed into rain and contribute to the overall precipitation bias in the model. The question of where this positive humidity bias in the model comes from requires further investigation, including understanding the transport of humidity and the processes occurring in the boundary layer in the model.

To investigate whether the observations and MM5 reveal an additional effect on the remote forcing (SSTs in the central Pacific), other than the mean seasonal precipitation (i.e., wetter and drier than normal in 1997 and 1998, respectively), a cluster analysis was performed for the station data. The analysis was done using the k-means method, for the total number of rainfall events of both years, separately for region 1 and 2. This method minimizes the variance of the elements within each cluster, while maximizing the variance between the clusters. The analysis was performed with 34 events for region 1 and 40 for region 2, and tested for three, four, and five clusters. In region 1, the precipitation events can be grouped by their spatial distribution into four different type of events (see Fig. 12): type 1, uniform distribution in the region; type 2, precipitation only in the southern part of the region; type 3, precipi-

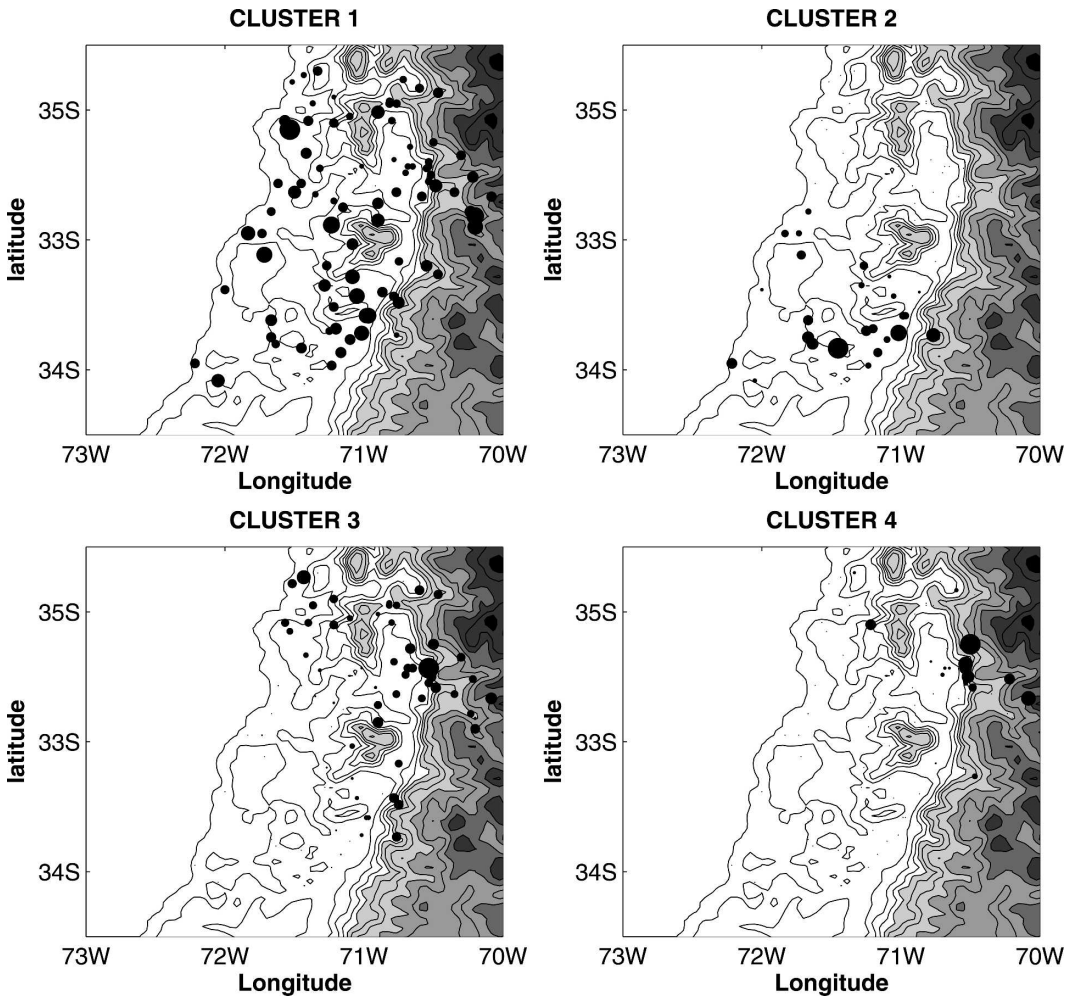

FIG. 12. Precipitation clusters of station data events in region 1.

tation localized in the cordillera region; and type 4, localized precipitation in the northern cordillera region.

In region 2 the clustering method did not find events sufficiently distinct to separate them into different classes; that is, most of the precipitation events had a uniform spatial distribution in the region. The more uniform distribution of precipitation in region 2 is probably because of the smoother topography in the region in comparison with region 1.

The same analysis was applied to MM5 domain 3 precipitation events in region 1. Clusters where calculated with 40 events (18 and 22 in 1997 and 1998, respectively) grouped into three, four, and five types of events. The clearest distinction between events is found when grouping these into four different types of events, and they are similar to the clusters obtained with the station observations (not shown). The population of the individual clusters is, however, different, with more events falling into the cordillera-only rain type event.

Separating the events by year reveals some distinct differences among them. In 1998 there are no uniform events, one-third of the events (5 out of 15) are southern events, another third is made up of localized events in the north-central part of the region, and the rest are local cordillera and local south events. In 1997 there were no localized cordillera events. All type of events, except those localized in the cordillera, have rain in region 2 as well.

5. Conclusions

The MM5 model has been run for two anomalous rainfall seasons in central Chile. The anomalously wet May–September 1997 and the anomalously dry May–September 1998 have been simulated to investigate the influence on rainfall of the model domain resolution, that is, the representation of topography in central Chile. The MM5, in the configuration used in this study,

captures the main features of rainfall and patterns of difference between the two simulated years. However, the main problem with the model is an overestimation of the precipitation (40%–80%). There are several factors that contribute to this bias. First, there is a bias in the content of water vapor in the model over the ocean when compared with boundary conditions (reanalysis fields). In addition, the precipitation bias is dependent on location. When comparing against higher-altitude stations, domains 2 and 3 exhibit larger biases (up to 120% for light rain, and 300% for heavy rain). A negative bias in daily extreme temperature is seen. These differences are correlated to the differences between station and model elevations (with a linear relationship). They probably are also a result of sampling error, as model output is available only every 6 h. Additionally, they could be influenced by the precipitation bias and other model physics. In particular, the model greatly overestimated the seasonal mean precipitation in 1998 in the northern part of central Chile (32°–35°S) (domain 1, 650%; domain 2, 525%; domain 3, 480%), so that the interannual differences are underestimated (1998 − 1997: 27%, 29%, and 33% in domains 3, 2, and 1 respectively, instead of the observed 9%). Too much rainfall in region 1 is because of two factors. Rainfall events reaching farther north than actually observed and unobserved rainfall in the Andes Cordillera in addition to the bias in water vapor content in the model, which is higher in 1998 than in 1997.

The problem of too much rainfall over mountainous areas remains an issue to investigate, not only for climate simulations but also for weather forecasting simulations. In preliminary work done to define the best configuration, a number of 1-month-long runs were performed, and the use of more complex microphysics parameterizations produced even more precipitation over the mountains.

Overall, domain 3, with a 15-km grid interval and therefore the best representation of the finescale topography, shows the best results, discarding precipitation above 1000 m. However, from a cost–benefit perspective, although a 15-km grid interval for a seasonal integration is affordable at the moment (computationally and in terms of storage), the improvements in the simulations are not very dramatic when compared with the cost. The simulation of important surface variables such as precipitation and temperature is greatly improved when downscaling from 135 to 45 km; however, smaller improvements are obtained when going down from 45 to 15 km. If climate studies on a longer time scale (e.g., for climate change studies) is the main interest, the results shown in this paper suggest that a horizontal grid interval of 40–30 km would be sufficient to capture the important climatic controlling factors of the region. Finally, any application of a regional climate model for impact studies will have to carefully take into account the large precipitation bias at high altitude.

Acknowledgments. This investigation was supported by the FONDECYT (Grant 3020039). Thanks to the Dirección General de Aguas and Dirección Meteorológica de Chile for providing the station data used in the validation of the simulations. Thanks to Rodrigo Sanchez and Mark Falvey for computing and software support and discussion of the results. I also thank Anji Seth and Filippo Giorgi and two anonymous reviewers for very useful comments on the manuscript.

REFERENCES

Aceituno, P., 1988: On the functioning of the Southern Oscillation in the South American sector. Part I: Surface climate. *Mon. Wea. Rev.,* **116,** 505–524.

Adler, R. F., and Coauthors, 2003: The version-2 Global Precipitation Climatology Project (GPCP) monthly precipitation analysis (1979–present). *J. Hydrometeor.,* **4,** 1147–1167.

Arnell, N. W., D. A. Hudson, and R. G. Jones, 2003: Climate change scenarios from a regional climate model: Estimating change in runoff in southern Africa. *J. Geophys. Res.,* **108,** 4519, doi:10.1029/2002JD002782.

Chen, F., and Coauthors, 1996: Modeling of land surface evaporation by four schemes and comparison with FIFE observations. *J. Geophys. Res.,* **101D,** 7251–7268.

Departamento de Geofísica, cited 2005: *Boletin Climático*. Departamento de Geofísica, Universidad de Chile. [Available online at http://met.dgf.uchile.cl/clima/.]

Dudhia, J., 1989: Numerical study of convection observed during the Winter Monsoon Experiment using a mesoscale two-dimensional model. *J. Atmos. Sci.,* **46,** 3077–3107.

——, 1993: A nonhydrostatic version of the Penn State/NCAR mesoscale model: Validation tests and simulation of an Atlantic cyclone and cold front. *Mon. Wea. Rev.,* **121,** 1493–1513.

Fuenzalida, H., 1982: A country of extreme climate. *Chile: Essence and Evolution* (in Spanish), H. Garcia, Ed., Instituto de Estudios Regionales, Universidad de Chile, 27–35.

García-Huidobro, T., F. Marshall, and J. Bell, 2001: A risk assessment of potential crop losses due to ambient SO_2 in the central regions of Chile. *Atmos. Environ.,* **35,** 4903–4915.

Giorgi, F., X. Bi, and J. Pal, 2004: Means, trends and interannual variability in a regional climate change experiment over Europe. Part I: Present day climate (1961–1990). *Climate Dyn.,* **22,** 733–756.

Grell, G., L. Schade, R. Knoche, A. Pfeiffer, and J. Egger, 2000: Nonhydrostatic climate simulations of precipitation over complex terrain. *J. Geophys. Res.,* **105,** 29 595–29 608.

Hack, J. J., B. A. Boville, B. P. Briegleb, J. T. Kiehl, P. J. Rasch, and D. L. Williamson, 1993: Description of the NCAR Community Climate Model (CCM2). NCAR Tech. Note NCAR/TN-382+STR, 108 pp.

Instituto Nacional de Estadísticas, cited 2005: CHILE: Censo de

poblacion y vivienda 2002. Instituto Nacional de Estadísticas, Santiago, Chile. [Available online at http://www.ine.cl/redatam/i-redatam.htm/.]

Kain, J. S., and J. M. Fritsch, 1993: Convective parameterization for mesoscale models: The Kain–Fritsch scheme. *The Representation of Cumulus Convection in Numerical Models, Meteor. Monogr.,* No. 46, Amer. Meteor. Soc., 165–170.

Kalnay, E., and Coauthors, 1996: The NCEP/NCAR 40-Year Reanalysis Project. *Bull. Amer. Meteor. Soc.,* **77,** 437–471.

Miller, A., 1976: The climate of Chile. *Climates of Central and South America,* W. Schwerdtfeger, Ed., Elsevier, 113–145.

Montecinos, A., and P. Aceituno, 2003: Seasonality of the ENSO-related rainfall variability in central Chile and associated circulation anomalies. *J. Climate,* **16,** 281–296.

Pizarro, J. G., and A. Montecinos, 2000: Cutoff cyclones off the subtropical coast of Chile. Preprints, *Sixth Int. Conf. on Southern Hemisphere Meteorology and Oceanography,* Santiago, Chile, Amer. Meteor. Soc., 278–279.

Rutllant, J., and H. Fuenzalida, 1991: Synoptic aspects of the central Chile rainfall variability associated with the Southern Oscillation. *Int. J. Climatol.,* **11,** 63–76.

Seth, A., and M. Rojas, 2003: Simulation and sensitivity in a nested modeling system for tropical South America. Part I: Reanalyses boundary forcing. *J. Climate,* **16,** 2437–2453.

Small, E. E., F. Giorgi, and L. C. Sloan, 1999: Regional climate model simulation of precipitation in central Asia: Mean and interannual variability. *J. Geophys. Res.,* **104,** 6563–6582.

Troen, I., and L. Mahrt, 1986: A simple model of the atmospheric boundary layer: Sensitivity to surface evaporation. *Bound.-Layer Meteor.,* **37,** 129–148.